

THE LAUNCH LOOP: A LOW COST EARTH-TO-HIGH-ORBIT LAUNCH SYSTEM

by Keith H. Lofstrom keithl@ieee.org

Note: This paper was first given at the 1985 AIAA conference referred to in the reference. A more up-to-date description of the Launch Loop can be found at www.launchloop.com.

ABSTRACT

The Launch Loop is an Earth-surface-based launching utility that stores energy and momentum in a very long, small cross-section iron ribbon loop moving at high velocity. The downward forces necessary to deflect the ribbon from its otherwise straight path support a magnetically-levitated track system, control cables, and vehicles at high altitudes against gravity. This paper presents a preliminary system that can launch five metric ton vehicles to geosynchronous or near-lunar orbits at rates of up to 80 per hour.

1. Introduction

Rockets are expensive. Rockets must carry enormous fuel supplies, and intricate engines that operate at high power levels for brief periods. Even with partial re-use of a launch system, staging discards a lot of costly equipment. The long turn-around times for the re-usable components suggest a long payback period for the initial investment and long idle times for most of the ground components of the system. The low frequency of launches, and the differing nature of each one, require a high degree of expertise from the launch operators and increase the chance of costly, time-consuming errors.

It is difficult to imagine how larger rocket systems requiring larger facilities, longer development times, and new technologies [1] can improve the picture. Rocket launch costs will certainly improve with increased usage, but the costs may never drop low enough to make large scale space industry and space colonization practical. Alternatives to the rocket are necessary.

Proposed schemes for electromagnetic launch from the Moon [2] or from the Earth [3] involve very high accelerations suitable only for raw materials. The high peak power circuitry may prove very expensive. Orbital capture systems must be constructed from large amounts of mass already in orbit [4,5,6], or require material strengths not yet available [7].

Accelerating a vehicle to 11 km/sec (the ΔV required to launch from the Earth's surface to L5 or the Moon) at 3 g's requires an acceleration path of 2000 km. The energy necessary is modest, about 60 MJ/kg. If provided at 100% efficiency from electricity costing 6 cents per kWhr, this energy costs about one dollar per kg. The Earth itself may provide the reaction mass.

The Launch Loop [18,19] provides vehicle energy and momentum more efficiently than rockets, but uses simpler vehicles. The Launch Loop is based on the ballistics of high speed continuous flows of materials and electronically-controlled ferromagnetic levitation. The ribbon supports and drives the system with its inertia, and is segmented to prevent axial tensions. The materials required to build the Launch Loop are commercially available in large quantities.

2. Dynamic Structures

Imagine a stream of water from a hose pointed at an angle into the sky. Neglecting effects of air friction, the stream forms a continuous parabolic arc, the ballistic trajectory of the individual particles in the

stream. If the stream of water is moving very fast when it leaves the hose, the height of the trajectory and the distance it traverses are well beyond what can be constructed with ordinary materials. If a flat plate is brought up against the stream at a slight angle downward, the stream is deflected downward, putting an upward force on the plate. In this way, the moving stream may be used to support a stationary weight.

If the stream is surrounded by a frictionless hose, the downward deflection of the stream may be used to support the weight of the hose. When the stream reaches the ground at the end of its trajectory, it may be deflected back toward its source, and deflected forward again, completing the loop. If the hose is truly frictionless, large, apparently static structures may be built.

If the stream is replaced with a ribbon of iron, and the hose is replaced by a track, the two may be held together magnetically, with a magnetic pressure of $B^2/2\mu_0$ [8]. The inertia of the iron ribbon supports the structure, but the ribbon sustains no axial stresses. This allows tall structures to be built unhindered by conventional strength-of-materials limits.

3. The Launch Loop

A highly schematic view of the Launch Loop is shown in Figure 1.

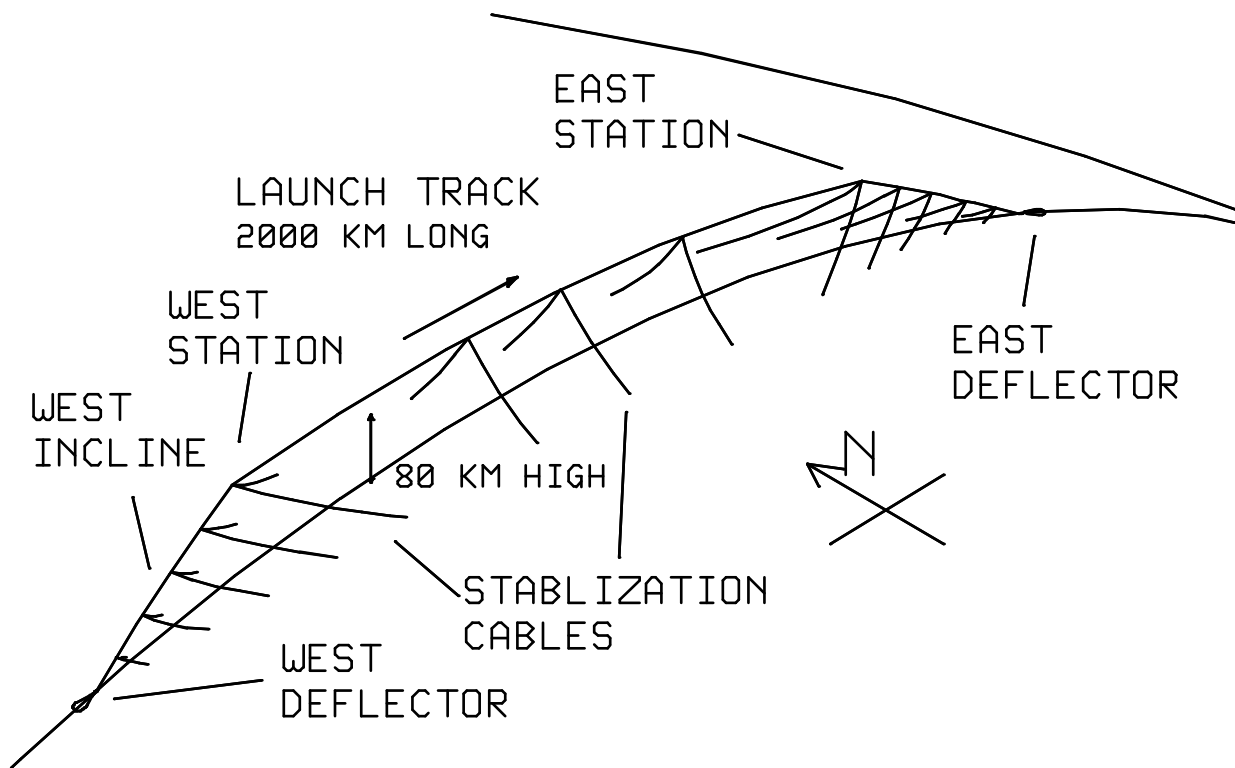


Figure 1. A side view of the Launch Loop. Most cross sections are in centimeters, making the structure virtually invisible from a distance.

The Launch Loop is a long, small cross-section structure built around a laminated, segmented iron ribbon loop moving at 14 km/sec. The ribbon is 5 centimeters wide and 7.6 millimeters thick. This ribbon

circulates around the system once every six minutes, travelling around the ends, up the inclines, down the launch path, then down the incline at the other end. When the ribbon reaches the far end of the Launch Loop, it is deflected 180° and returned to complete the cycle.

Large forces are required to deflect the moving ribbon. These forces support a *non-moving* track system of cables, control electronics, and permanent magnets by ferromagnetic attraction.

At the top of the Launch Loop is the 2000-km long launch path. Vehicles riding magnetically on the forward ribbon of the launch path are accelerated at 3 g's to reach ground-relative transfer orbit velocities up to 10.5 km/s. Small payloads may be pushed faster.

The launch path track is suspended on permanent magnets one centimeter below the iron ribbon. The launch path track supports sensor and control electronics packages, as well as parachutes to protect sections of track from catastrophic system failure.

The ribbon and static track structure of the launch path weigh about 3 kg/m and 4 kg/m respectively, and are shown in Figure 2.

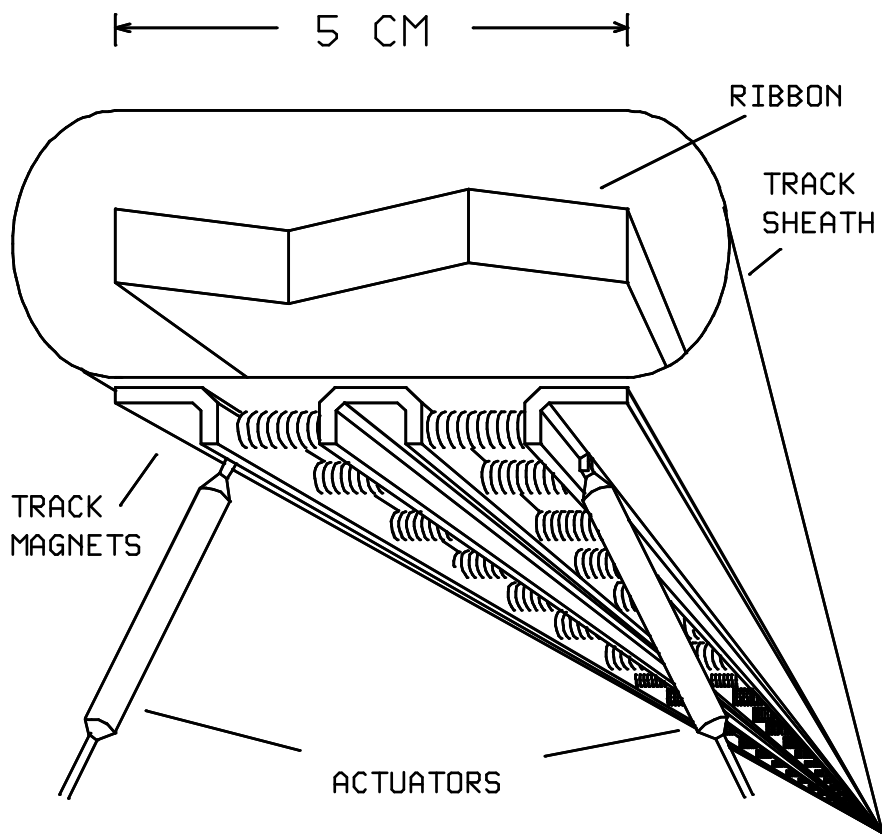


Figure 2. A cross section of the ribbon and track.

In front of and behind the launch path are the inclines, which slope down to the surface at angles of 9 to 20 degrees. The forward and reverse ribbons of the inclines are surrounded by lightweight vacuum sheaths.

The inclines are much heavier than the launch path track. Anchor cables control the sections against wind, and the track must support an airtight sheath and vacuum pumps. To compensate for the extra

weight, the inclines curve more than the Earth's surface. The tension on the inclines is relieved by diagonal cables to the surface.

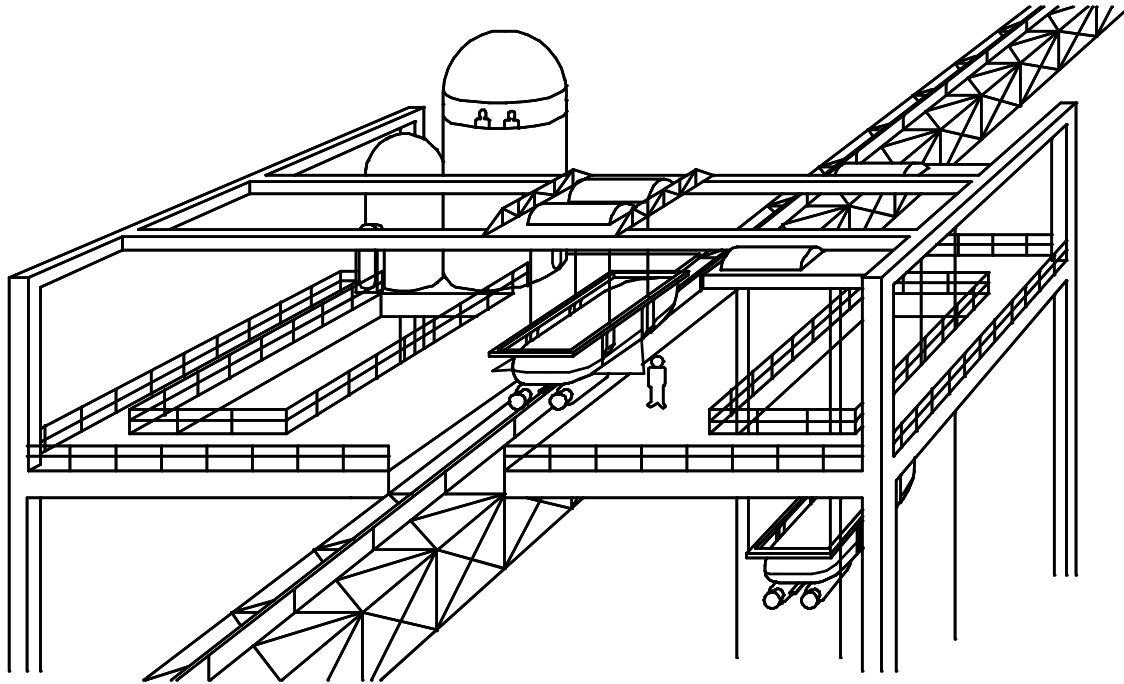


Figure 3. West station, showing a vehicle being loaded onto the track.

The inclines and the launch path are joined by two curved, 5000-metric-ton deflector sections containing magnets, control systems and elevators from the surface. The upper deflectors are referred to as the "east" and "west" stations; vehicles are hauled up to west station and launched from there. West station is illustrated in Figure 3.

The long elevators to the stations are supported by pulleys from the anchor cables. The vehicles are brought up these cables rather than up the west incline to simplify the spacing controllers on the incline. Other benefits of this approach are minimized incline weight, shorter upward transit times, and less likelihood of sheath damage.

Near the Earth's surface, each incline ends at a curving ramp with magnets that deflect the ribbon to or from the horizontal plane. Once the ribbon is horizontal, it is twisted on its length axis 90° so that the broad surface points at the horizon. The ribbon is then deflected 180° in the horizontal plane by a large, flat semicircular section (14 km radius) of high-energy magnets. The windings for the linear motors that drive the ribbon are positioned between the semicircular sections and the upwards ramp on the east end. The ribbon is then twisted back to flat, and sent back west through the system to complete the loop. The east end of the Launch Loop is shown in Figure 4.

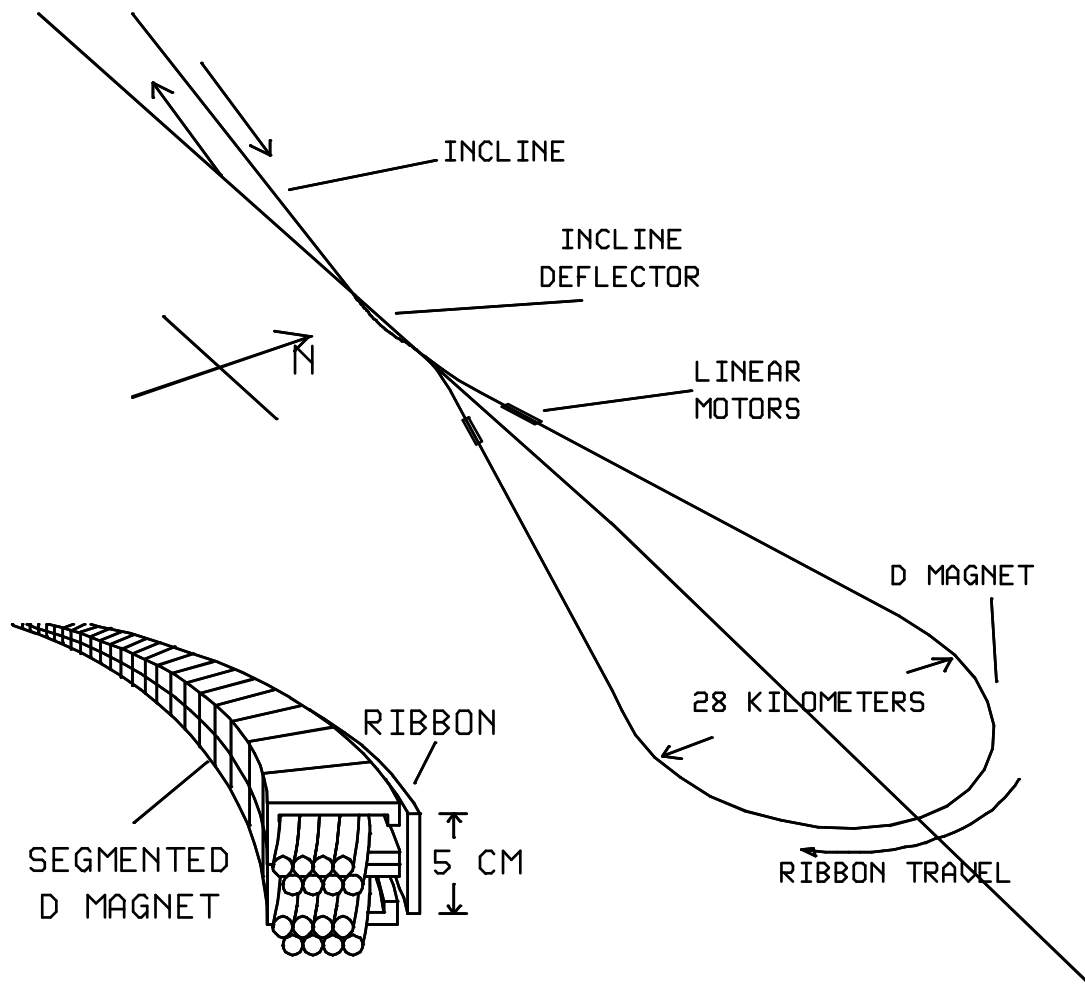


Figure 4. The east end deflectors, motors, and the start of the east incline. The inset shows a section of deflector magnet.

The Launch Loop is located on the equator to minimize vehicle apogee ΔV as well as weather and Coriolis effects. For safety and ease of construction, the system is located over the ocean, far from land. This means increased shipping costs from northern hemisphere industry, increased corrosion, and long anchoring cables to the deep sea bed. These drawbacks are balanced by the ability to start the Launch Loop from a relatively flat surface, and move the various deflectors during construction.

The sloping sheath and cables are subject to wind loading in the lower atmosphere, although most of the system is in near vacuum. The sudden loads caused by wind gusts cause extra stress on the structure, and the static loading of steady winds distort the structure and contribute inaccuracies to vehicle trajectories.

Assuming a drag coefficient of 0.5, a 100-knot sea level wind places a 50 N/m load on a 10-cm-diameter sheath, as would a 200-knot wind at the 250-mbar level of the atmosphere. A sheath with a rotating airfoil shape may cut the drag coefficient by a factor of 10 or more.

Equatorial winds tend to be unpredictable and vary greatly with altitude [12], but their maximum speeds are relatively low and the lack of Coriolis force inhibits cyclones. The most severe stresses can be

expected during squalls, whose maximum winds cannot be forecast with present techniques. The equatorial site should be chosen with measured wind history in mind, so that the system survives normal storm conditions.

4. System Startup

The Launch Loop is started floating on the surface of the ocean, at rest. Startup imposes some of the most severe stresses on the system, as the launch track is now on the surface and must be protected by a temporary sheath that can stand off a full atmosphere. In addition, the control system must compensate for ocean wave forces. During this time, the track and magnet system is supporting the ribbon, not vice versa; the system is started with the track upside down.

The ribbon is started, slowly at first, by pulling on it with motors at the ends of the Loop. Given the enormous inertia of the ribbon, and the weak joints that separate the ribbon segments, the initial acceleration is about 1 cm/sec^2 . At this acceleration, it takes 9 hours just to make one pass of the ribbon through the motors, and 3 days before the motors can work at full power.

The ribbon weighs 15,600 metric tons; accelerating it to 14 km/sec requires 1.5×10^{15} Joules of kinetic energy. If this energy is put in at a 300 Mw rate, the system requires 60 days to reach full speed, while the Loop is flat on the surface. For a Loop operation at this power level, it may be practical to temporarily attach 1 Gw of gas turbines on floating barges to start it up more quickly.

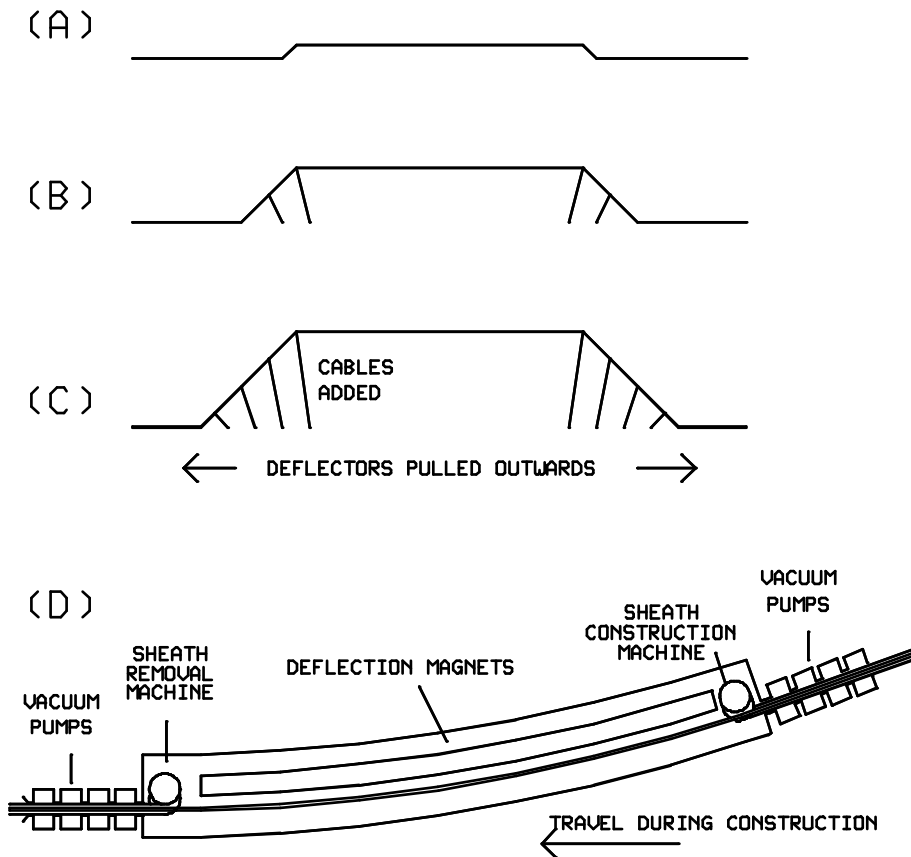


Figure 5. Starting up the Launch Loop. (a) up to speed, flat on the surface. (b) partially raised, with the ramps pulling towards the ends. (c) fully erected, the track sheath being stripped away. (d) the west end incline deflector during erection.

The startup process is illustrated in Figure 5. At startup time, the east and west stations are near the surface. The deflection ramps are temporarily pulled 300 km inwards, and are located next to the stations.

When the system is up to speed, the stations are raised out of the water by increasing the curvature of the surface incline deflectors and the tension in the station anchor cables. The ribbon is now being deflected 5 degrees at the incline deflectors and at the station; the distance from incline bottom to station top is 100 meters.

The system is brought to altitude by slowly drawing the surface incline deflectors away from the stations. New sheath is constructed around the slowly-growing inclines and removed from the long sections between the inclines and the end deflectors. Cables are added to the inclines as necessary. If automatic construction machinery is capable of producing 20 meters of sheath per minute, the erection process should take about 10 days.

When the system finally reaches 80 km altitude, the temporary sheath is cut away along the entire length of the launch track. Segments of the temporary sheath sections are lowered down the station cables. The launch track stabilization cables are tightened to make up for the lost weight of the sheath.

5. Dynamics of the High Speed Ribbon

The ribbon will be analyzed assuming a uniform weight per length m_r , without tensile or bending forces. Lower case m is used for distributed masses, while upper case M is used for point masses. A ribbon moving at a speed of V_r may be deflected by an angle Θ with a force of:

$$F = 2 m_r V_r^2 \sin(\Theta/2) \approx m_r V_r^2 \Theta \quad (1)$$

The ribbon speed does not change; just the direction of the velocity vector.

A distributed force can deflect the ribbon as well. For example, a ribbon constrained to follow the curvature of the Earth requires a distributed force to hold it to the curved path. If the ribbon is moving at circular orbital velocity, the deflection force is equal to its weight. If it is moving faster than orbital velocity V_o , deflecting it to follow the curve of the Earth requires an external downward force per length of

$$f = a_g m_r \left(\left(\frac{V_r}{V_o} \right)^2 - 1 \right) \quad (2)$$

The prograde surface-relative orbital velocity at 80 km altitude is about 7400 m/s. A ribbon moving at a surface-relative velocity of 14 km/s and weighing 3 kg/m requires an external downwards force of 68.5 N/m. This force can be provided by the weight of a non-moving track weighing 7.1 kg/m. The same ribbon moving retrograde can support 5.9 kg/m of stationary track.

The Launch Loop ribbon is constrained to rise and fall as it travels around the system, changing altitude by 80 km in the process. The ribbon moves faster at ground level because it is accelerated by gravity on the way down from 80 Km and decelerated on the way up. The higher ground velocity of 14,055 m/s requires that the ribbon stretch by 0.4%. The mass density is lower by the same amount. To accommodate this stretch, the ribbon may be constructed out of two-meter-long segments connected with sliding joints.

The axial acceleration of the ribbon requires large amounts of force and power. If the ribbon velocity is increased by ΔV , the necessary force is:

$$F = m_r V_r \Delta V \quad (3)$$

A 14 km/s, 3 kg/m ribbon is slowed 3.6 m/s by a force of 150 KN. This force can be used to accelerate a 5000-kg space vehicle at 3 g's. Force is provided purely by the deceleration of the ribbon, and does not necessarily result in any stress on the ribbon.

The power evolved by decelerating the ribbon is given by:

$$P = m_r V_r^2 \Delta V \quad (4)$$

For the ribbon parameters given, the power is 2.1 Gw. Part of this power is turned into payload kinetic energy, and part of it appears as waste heat in the ribbon.

6. Magnetic Deflection of a Moving Ribbon

The ribbon may be coupled to the track by ferromagnetic attraction or eddy current repulsion. Ferromagnetic attraction is the well known attraction between magnets and iron. Eddy current repulsion is based on the diamagnetic properties of moving conductors.

Eddy currents are produced by changing the magnetic flux through the ribbon. These currents force the flux out of the ribbon and generate repulsive forces. Eddy current repulsion is being considered for some magnetic levitation train designs [8] because the system is more stable and the track is cheaper. It's main drawback in this application results from the limited conductivity of elevated temperature conductors. Aluminum has the best conductivity per weight of any normal metal, but the high currents necessary to generate lift result in resistive losses of hundreds of watts per meter. This results in an unacceptably large standby dissipation for the Launch Loop.

Ferromagnetic attraction is unstable, but this effect can be masked electronically. A control winding can also compensate for vehicle-induced transients. With a spacing of 1 cm, one may expect a magnet lift-to-weight ratio of 3 or better. The control winding dissipation is minimized by using permanent magnets, but some power is lost correcting perturbations. If the winding power is 80 mw/N in the track and 15 mw/N in the semicircular deflectors and the east and west stations, the power dissipated in the windings is 35 and 90 Mw respectively. Variations of magnetic field in the track also induce eddy currents and drag in the ribbon.

7. Stability of a Magnetically Deflected Ribbon

Attractive magnetic levitation is unstable. If the current to the electromagnet inducing the magnetic field is constant, moving the levitated body closer to the magnet decreases the gap, resulting in an increased magnetic field. The increased field results in increased force, accelerating the levitating body towards the magnet even faster. In the Launch Loop, this instability is corrected by electronically controlling the winding currents in short segments of the deflector magnet.

The fl at ribbon can rotate axially, and this doubles the computational load. The control of each edge closely approximates the control of a separate non-rotating ribbon of half the width, so the following analysis will be made using this approximation. Side-to-side shifts are restored by the divergence of the track magnetic field.

The most difficult control problem is the D deflector magnets at the ends of the Loop. Assuming a ribbon speed of 14 km/s, and a deflector radius of 14 km, the deflection acceleration on the ribbon is 14,000 m/s², or 1430 g's. If the nominal gap between the magnet and the ribbon is 1 mm, a perturbation of only 1 μm results in a perturbation acceleration of 28 m/s², which increases the perturbation still further. For the parameters given, perturbations double every 180 microseconds, or every 2.5 meters of travel down the deflector.

Over shorter distances, the ribbon can buckle. The ribbon stiffness resists perturbations with wavelengths less than 30 cm, but longer wavelength perturbations grow exponentially. This "stiffness wavelength" determines the number of control points per meter, while the perturbation growth time determines the time sample rate. If the perturbations grow slowly, the same control values may be shifted to many succeeding controllers, saving computational hardware.

Both these effects are driven by the variation of the magnetic field with gap spacing, which is given by:

$$B = \frac{\mu_0 I}{2g} \quad (5)$$

μ_0 is the permeability of free space, I is the effective current in the electromagnet winding in amp-turns, and g is the gap in meters. The flux passes through the gap twice, into and out of the ribbon. The magnetic pressure $B^2/2\mu_0$ produces an attractive force between the two poles of the magnet and the iron ribbon of:

$$f = \frac{W_P B^2}{\mu_0} = \frac{W_P \mu_0 I^2}{4g^2} \quad (6)$$

where W_P is the width of the magnet pole.

The ribbon has a mass per length of m_r , resulting in a magnetic centrifugal acceleration of:

$$a = - \frac{W_P \mu_0 I^2}{4m_r g^2} \quad (7)$$

With a nominal gap g_0 and the correct control current I_0 , the magnetic centrifugal acceleration is $-a_0$, where a_0 is equal to the centrifugal acceleration of the ribbon around the deflector.

$$a_0 = \frac{W_P \mu_0 I_0^2}{4m_r g_0^2} \quad (8)$$

Assume a fixed deflector (not always a good assumption!) and small perturbations \hat{z} from nominal gap g_0 . This calculation is performed in a moving frame of reference $\hat{x} = x - V_r t$ following the ribbon. The change in centrifugal acceleration with gap is given by:

$$\frac{\partial a}{\partial \hat{z}_r} = \frac{W_P \mu_0 I^2}{2m_r g^3} \approx \frac{W_P \mu_0 I_0^2}{2m_r g_0^3} \approx \frac{2a_0}{g_0} \quad (9)$$

By a similar argument, the acceleration changes with control current as

$$\frac{\partial a}{\partial I} \approx -\frac{2a_0}{I_0} \quad (10)$$

The acceleration is simply the second derivative of \hat{z}_r . For small perturbations, the local equation of motion is thus:

$$\frac{d^2 \hat{z}_r}{dt^2} = \left(\frac{2a_0}{g_0}\right) \hat{z}_r \quad (11)$$

which has solutions of the form:

$$\hat{z}_r = \hat{z}_{r_0} e^{\pm(t/\tau)} \quad \tau \equiv \left(\frac{g_0}{2a_0}\right)^{\frac{1}{2}} \quad (12)$$

The doubling time for the perturbation is $(\tau \ln 2)$.

If the stiffness of the ribbon in the \hat{x} direction is included, a more complex picture emerges. The stiffness introduces the bending force f_b :

$$f_b = -E_{FE} I_b \frac{\partial^4 \hat{z}_r}{\partial \hat{x}^4} \quad (13)$$

E_{FE} is Young's modulus for the iron ribbon, and I_b is the bending moment, which is given by:

$$I_b = \frac{W \delta^3}{12} \quad (14)$$

for a flat ribbon with a width of W and a thickness of δ . Other cross sections, such as crescents, I's, and hollow cylinders have a larger bending moment, and a more optimal (but harder to analyze) Launch Loop may be built around these.

The mass of the strip is given by $m_r = \rho_{FE} W \delta$. The longitudinal speed of sound in the material is:

$$C_{FE} \equiv \left(\frac{E_{FE}}{\rho_{FE}}\right)^{\frac{1}{2}} \quad (15)$$

The acceleration, which is the force divided by the mass, is given by:

$$a_b = -\left(\frac{C_{FE}^2 \delta^2}{12}\right) \frac{\partial^4 \hat{z}_r}{\partial \hat{x}^4} \quad (16)$$

The differential equation describing the ribbon is thus:

$$\frac{\partial^2 \hat{z}_r}{\partial t^2} = \left(\frac{2a_0}{g_0}\right) \hat{z}_r - \left(\frac{C_{FE}^2 \delta^2}{12}\right) \frac{\partial^4 \hat{z}_r}{\partial \hat{x}^4} \quad (17)$$

This equation can be solved with Fourier analysis. Assume that:

$$\hat{z}_r = \hat{z}_{r0} e^{i(\omega t - kx)} \quad (18)$$

where ω is the angular frequency and k is the wavenumber, related to the wavelength by $k = 2\pi/\lambda$. Equation (17) reduces to:

$$-\omega^2 = \left(\frac{2a_0}{g_0}\right) - \left(\frac{C_{FE}^2 \delta^2}{12}\right) k^4 \quad (19)$$

For $k = 0$, equation (19) implies the growth time of equation (12). As k gets larger (or equivalently, the wavelength gets shorter), the imaginary quantity ω tends towards zero as the growth time gets larger. For long wavelengths, ω is real and the solutions do not grow with time. The system is stable, and dispersive; wave packets on the ribbon spread out over time.

Since $\lambda = 2\pi/k$, the condition of stability becomes:

$$\lambda < 2\pi \left(\frac{g_0 C_{FE}^2 \delta^2}{24a_0} \right)^{1/4} \quad (20)$$

For the parameters mentioned above, equation (20) yields a wavelength of 31 cm. Sampling theory suggests the control sections should be no longer than half this wavelength, or 15 cm. The filtering job is easier if the sections are smaller still, perhaps 10 cm long. A stiffer ribbon, perhaps with a different shape, results in a longer λ , requiring less control sections per meter.

8. The D Magnet Digital Controller

What magnitudes of currents and voltages must the controller handle? This is dependent on the size of the perturbations, of course; if the system is well behaved, they are zero. Control sections can fail, however, and introduce perturbations as large as the limits of their control range. Thus, the larger the control range, the more control range is needed to correct. This is not a problem if the percentage of failed sections is kept small.

Assume a sinusoidal variation in spacing moving with the ribbon, with an amplitude of $\pm 100 \mu\text{m}$, and a wavelength of 0.4 m. From equation (10), the peak control current is $0.1 I_0$. The voltage can be computed from the change of energy and thus the flow of power in and out of a local section of magnet:

$$VI_0 = Power = \frac{\partial E}{\partial t} = V_r k f z \quad (21)$$

where z is the amplitude of the variation and f is the magnet force. The instantaneous power in a 10 cm section of magnet, for half the ribbon, is 15 kW. The local controller is handling 10% of the power. The rest of the power is handled by the main magnet controller. 1500 W per controller is quite a bit; while the controllers need not dissipate this much power continuously, they must be able to stand off this voltage-current product. Many semiconductor devices are able to stand pulse currents that are some multiple of their DC rating. These devices handle high-current pulses less than 100 microseconds long; devices with DC power ratings of 300 watts are probably adequate.

The control range allowed by the local controllers lets them correct a perturbation of up to $0.1 g_0$, or $\pm 100 \mu\text{m}$. This amount of perturbation can be caused by the preceding 4 meters of control section being stuck on (40 control sections), or by an uncorrected perturbation of $2 \mu\text{m}$ up to 7 meters away. Obviously, the preferred failure mode for a controller is off, rather than stuck on; this can be achieved with current limiting shutdown circuits and fuses.

20 separately switched and fused control sections (10 for each side of the ribbon), each 10 cm long, make up a single one-meter-long control block. Each control block has its own group of optical position measurement stations and its own digital processor. The digital processor performs three multiplies and adds using the last three optical position measurements on each side of the ribbon, and generates 8-bit

values into a control lookup table. The table output is 16 bits wide, one bit for each on or off control section. The 32 bits are fed into shift registers, which deliver delayed control information to each control section as the measured portion of ribbon passes it. This process is repeated at a 340 kHz rate. The 1 million multiplies per second can be easily performed by a small, 3-micron technology CMOS integrated circuit.

Central host computers program the controller lookup tables and multiplication constants over communication buses. These constants are computed from the state of the Launch Loop system, including controller failures. There are approximately 150 km of D magnets in the Launch Loop system; 150,000 of these controllers are needed. Total computation rate for the sum of all controllers is 150 billion multiply and adds per second.

Each one-meter control section must handle 30 kw peak, which should cost about what a 6 kw average switching power supply would cost in very large quantities. Prices of \$0.10 per average watt are not too unlikely for tested and installed controllers. The digital controller and sensors may cost \$200, for a per-unit controller cost of \$800.

9. Low Acceleration Sections

The incline sections and launch track support only their own weight, and deflect the ribbon more gradually than the D magnets at the end of the Launch Loop. The lower forces and wider spacings involved allow widely spaced track controllers that use less power than their equivalents on the D magnets.

Unlike the D magnets, however, the track is not solidly anchored to the ground, and is far lighter. This results in a more complex mathematical description. The absolute position of the track is harder to determine since it is much farther from any ground reference. This requires higher accuracy measurements and calculations.

There are two z values to account for; z_r for the ribbon and z_s for the horizontally stationary track. The stiffness of the track is important, and due to its complex nature, is harder to compute. The track is under tension, which adds terms to the descriptive equations.

Define z_r as the deflection of the ribbon from nominal position, and z_s as the difference between normal and perturbed track position. The track and ribbon are normally spaced about 1 cm apart. The position in the moving frame is \hat{x} , where:

$$\hat{x} = x - V_r t \quad (22)$$

The z position of the ribbon in the moving frame is \hat{z}_r . The forces pulling down on the ribbon are:

$$f = -m_r \frac{\partial^2 \hat{z}_r}{\partial t^2} - EI_r \frac{\partial^4 \hat{z}_r}{\partial \hat{x}^4} - \left(\frac{2f_0}{g_0} \right) (z_r - z_s) \quad (23)$$

The left hand side of the equation is the "control force" that the controller manipulates by controlling magnet voltage and current. The first right-hand term is the kinematic term, and ribbon bending is accounted for by the second term, where EI_r is the ribbon stiffness. m_r is the mass-per-length of the ribbon.

The third right-hand term is the magnet instability term. g_0 is the nominal ribbon to track spacing, while f_0 is the nominal force per length. The characteristic time $\tau \equiv (g_0 m_r / 2f_0)^{1/2}$ is much longer than the τ of the D magnets; 30 milliseconds versus 180 microseconds. This means the controllers can be slower and spaced further apart.

Equation (23) can be expressed in fixed-frame coordinates as:

$$f = -m_r \left(\frac{\partial^2 z_r}{\partial t^2} - 2V_r \frac{\partial^2 z_r}{\partial x \partial t} + V_r^2 \frac{\partial^2 z_r}{\partial x^2} \right) - EI_r \frac{\partial^4 z_r}{\partial x^4}$$

$$-\left(\frac{2f_0}{g_0}\right)(z_r - z_s) \quad (24)$$

The track position equation is similar, but includes a tension term as well:

$$f = m_s \frac{\partial^2 z_s}{\partial t^2} + EI_s \frac{\partial^4 z_s}{\partial x^4} - \left(\frac{2f_0}{g_0}\right)(z_r - z_s) - T_s \frac{\partial^2 z_r}{\partial x^2} \quad (25)$$

The force is determined by the magnet controllers in the track. A typical track control equation is:

$$f = m_r(a_{rs}(z_r - z_s) + a_s(z_s)) \quad (26)$$

Where a_{rs} is a function of the position difference of the ribbon and track, while a_s is a function of absolute position of the track only.

Measuring the absolute track position is more costly than measuring the difference position - some form of laser interferometry may be needed. The functions should be chosen so that the a_s function is sampled far less frequently than the a_{rs} function.

Making the substitution $z = z_0 e^{i(\omega t - kx)}$, the above equations may be Fourier analyzed:

$$f = (m_r(\omega - V_r k)^2 - EI_r k^4) z_r - \left(\frac{2f_0}{g_0}\right)(z_r - z_s) \quad (27)$$

$$f = (-m_s \omega^2 + EI_s k^4 + T_s k^2) z_s - \left(\frac{2f_0}{g_0}\right)(z_r - z_s) \quad (28)$$

$$f = m_r(a_{rs}(\omega, k)(z_r - z_s) + a_s(\omega, k)z_s) \quad (29)$$

The mass ratio of the track to the moving ribbon is defined as $\mu \equiv m_s/m_r$. The magnet nonlinearity term is simplified with $\alpha_0 \equiv 2f_0/g_0$. The $V_r k$ term is replaced by $\omega_k \equiv V_r k$. Unless k is very large (that is, a very short wavelength) the bending terms can be ignored. The tension term modifies the character of the solution only slightly, so it is ignored for now. The above equations are further reduced to:

$$a_{rs}(z_r - z_s) + a_s z_s = (\omega - \omega_k)^2 z_r - a_0(z_r - z_s) \quad (30)$$

$$a_{rs}(z_r - z_s) + a_s z_s = -\mu \omega^2 z_s - a_0(z_r - z_s) \quad (31)$$

The following relation between z_r and z_s can be derived:

$$z_r = \frac{\mu \omega^2}{(\omega - \omega_k)^2} z_s \quad (32)$$

Equations (31) and (32) are combined, and the z_s term factored out:

$$\frac{a_{rs} + a_0}{a_s + \mu \omega^2} = \frac{(\omega - \omega_k)^2}{\mu \omega^2 + (\omega - \omega_k)^2} \quad (33)$$

Equation (33) is the characteristic equation for the track section. Since a_0 is not precisely known, and the a_{rs} term is a function of imperfect measurements, there is always a residual non-zero value for the left side of the equation. For large ω_k , equation (33) can be solved for four real roots, indicating solutions that propagate down the system, to be removed at a ground cable actuator. Unfortunately, as ω_k becomes small (or the wavelengths become large), two of the roots split and asymptote towards the complex poles defined by

$$\omega_p = \frac{1 \pm i\mu^{\frac{1}{2}}}{\mu + 1} \omega_k \quad (34)$$

One of the poles is unstable; unless the left-hand side of equation (33) is exactly zero, or the proper a_s and a_{rs} are chosen, long-wavelength perturbations grow with time as they propagate down-ribbon.

The problem is that the left side of equation (33) scales differently with ω_k than the right hand side, but this can be corrected with proper measurement and control. Damping factors can also be added to the control equations, making it possible to actually damp out perturbations. However, the damping factors must be chosen so that the measurements they depend on are possible to make - measuring absolute position of the track within microns is an example of an (at present) impossible measurement, while measuring acceleration may be less difficult.

One choice for control equations is:

$$a_{rs} \equiv \gamma \mu \omega_k^2 + c_1 \omega i + c_2 \omega_k i \quad (35)$$

and

$$a_s \equiv a_0 \left(\frac{\omega}{\omega_k} \right)^2 + c_4 \omega_k i \quad (36)$$

where γ is an arbitrary constant which determines the placement of the real part of the four roots of the system. If $\mu = 2$, a good choice for γ is 0.05. c_1 , c_2 , and c_4 are small constants chosen to make small, positive imaginary parts for the four roots. The $(\omega/\omega_k)^2$ term can be computed from sensitive accelerometer measurements.

Define $\xi \equiv \omega/\omega_k$, the normalized ω . There will be 4 roots for this fourth order system. Further define the function $f(\xi)$ as:

$$f(\xi) \equiv \frac{\xi^2 (\xi - 1)^2}{\mu \xi^2 + (\xi - 1)^2} \quad (37)$$

A plot of $f(\xi)$ will show double zeros at $\xi = 0$ and $\xi = 1$, and a local maxima in between. γ should be chosen between the local maxima and zero. If we set $\gamma = f(\xi)$, we will get four real roots in ξ . These will be the real parts of the normalized roots of the system.

If the imaginary parts of the roots are small compared to the real parts, equation (37) may be approximated by:

$$f(\xi) \approx \gamma + \frac{\partial f}{\partial \xi} \Delta \xi \quad (38)$$

Using equations (33) through (38) and ignoring some small terms, we arrive at the following equation for the small imaginary parts of the roots:

$$\Delta \xi \approx \frac{i \omega_k}{\frac{a_0}{\gamma} + \mu \omega_k^2} \frac{c_1 \xi + c_2 - \gamma c_4 / \xi^2}{\frac{\partial f}{\partial \xi}} \quad (39)$$

There are four $\Delta \xi$, one for each real root ξ . The control constants c_1 , c_2 , and c_4 may be chosen for robust, positive imaginary parts.

Other control functions are possible as well. The functions described here demonstrate that real-world solutions are possible, and give an idea of their complexity.

Knowing the approximate nature of the linear section controllers, their computational complexity can be determined. Assume the controllers are spaced 10 meters apart, and compute new control values for each two meter section every millisecond, for two sides of the ribbon. Assume the control algorithm involves 5 multiplies and adds for a fourth-order differential equation in time and second-order in space.

Each controller has 20 microseconds to do a multiply-add, which can be performed with a very simple serial architecture integrated circuit. 520,000 of these circuits are needed.

Power levels for the track-ribbon system are difficult to compute. As the area disturbed by the vehicle passes a section of track, the magnetic field, and the energy stored in it, must change. A rapid change in energy implies a large flow of power through the magnet control electronics. The magnitude of this burst of power, and its duration, determine the power rating necessary for the controller.

If some of the vehicle deflection forces are coupled directly to the track, rather than just the ribbon, the amount of work done by the spacing control electronics may be reduced. Similarly, the passage of dc magnets on the vehicle past stationary windings on the track can also be used to drive the spacing control magnets. These and other schemes for reducing the power level in the spacing control magnets must be both failsafe and not add greatly to vehicle cost.

The magnetic field in the disturbed region tends to propagate to the front or the disturbed region, carried along by the induced currents in the ribbon. The amount of this propagation is determined by the design, and determines how much extra field must be provided by the control electronics, and how much they cost.

The most magnetic force is needed when the vehicle is about to leave the ribbon and is moving about 11 km/s in relation to the track. The magnetic energy stored in the gap between ribbon and track must increase by 25 Joules per meter. Some of this energy is "pulled along" by the ribbon and some must be provided by the track control coils. With about 2 milliseconds to provide the energy, a high power rate is needed.

At the other end of the disturbance region of the track-ribbon system, the field energy must be drained away and the spacing forces restored to normal. Again, a high power rate may be needed, unless the energy in the track-ribbon system is made to propagate at the same speed as the vehicle.

Assume that the disturbance is made to propagate with 80% efficiency. The electronic devices in the controllers must handle 5 Joules per meter in 2 milliseconds. 2500 watts of peak-power handling is needed per meter. This is equivalent to about 1000 watts per meter of DC device power rating, or about \$100 of power handling controllers per meter of system track.

Only the last 500 km of track require expensive, high-power controllers. This section of track has the highest energy rate-of-change, because the vehicle moves fastest and needs high hold-down forces here. The rest of the track can be made with the same low-power controllers used by the retrograde ribbon and in the inclines.

10. Ribbon Design for the Launch Loop

The core of the Launch Loop is the ribbon; its properties control the design of the rest of the system. The ribbon is made with sliding segments to prevent tension from building up in the structure.

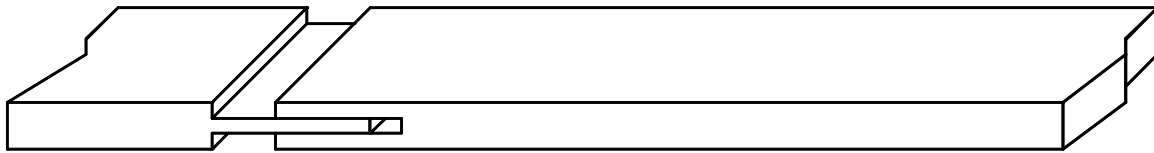
The necessary properties of the ribbon are:

- High electrical resistance path for high drag during vehicle launch.
- Low electrical resistance path for linear induction motor currents.
- $\pm 3\%$ stretch allowed by expansion joints.
- Tolerance of vibrations generated by vehicle magnets.
- High permeability path for deflection magnet flux.
- High stiffness perpendicular to the plane of the ribbon, to minimize flexing, and thus the number of control sections in deflection magnets.
- High axial strength, when extended, to speed Loop startup.

- Inexpensive manufacture from common materials.

The present design assumes a ribbon constructed with 2-meter-long segments separated by sliding joints. The segments are made from flat laminations of transformer iron separated by high-temperature insulation. A typical segment is pictured in Figure 6a. A complete Launch Loop uses 2.6 million of these segments.

(A)



(B)

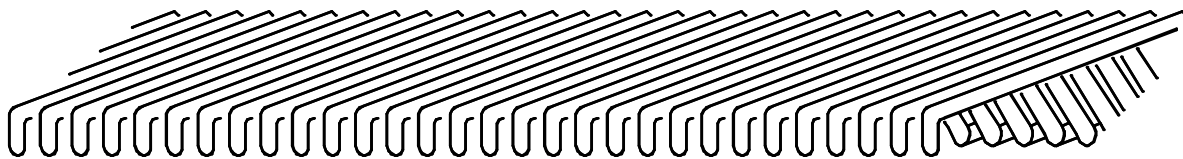


Figure 6. a) Joint for a 2 meter ribbon segment. b) Alternative ribbon construction from woven iron wire.

Another promising approach involves a ribbon made from woven iron wire. The wire may be woven to increase the penetration of magnetic fields into the ribbon, yet provide high conductivity paths for the drive motor. The wire loops in such a scheme have a characteristic wavelength, and systems of alternating magnets with different pole spacings will see different effective impedances. This allows the vehicle magnets to see a much higher impedance than the linear induction drive motors do, providing for high vehicle accelerations. It may be difficult to stiffen such a ribbon against bending, however.

11. Anchor Cables and Structural Shape

The Launch Loop is supported by the deflection of the moving ribbon; its shape is maintained by weights and anchor cables. The long cables are tapered, and thicker at the top than at the bottom, for a constant stress per area. This allows the use of presently available materials. The characteristic length (or support length) H_c of the cable material is defined as $H_c \equiv Y/a_g \rho$, where Y is the strength per area, a_g is the gravitational acceleration, and ρ is the density. Kevlar® fiber yarn has a tensile strength of 2.7 Gigapascals, and a density of 1440 kg/m³ [9], for a raw characteristic length of $H_c = 191$ km. The Kevlar cables used here are 40% epoxy-filled by weight, and have a safety factor of 1.5, resulting in a characteristic length of $H_c = 80$ km.

The long cables run diagonally to the ground. Due to their gradual taper, they do not follow a catenary curve. The horizontal tension force remains the same with altitude; the vertical force increases as:

$$T_z = T_x \left(e^{\frac{2(z+z_0)}{H_c}} - 1 \right)^{\frac{1}{2}} = T_x G(z) \quad (40)$$

where z_0 is chosen to give the proper angle at the bottom of the cable.

The tension in the sheath is proportional to the change in vertical height. This force may be periodically relieved by cables running diagonally off the track/ribbon system. The cables deflect the ribbon down and generate horizontal forces that can relieve the forces in the sheath.

For example, assume a stress relief anchor cable from 70 km altitude, and that $z_0 = 20$ km and $H_c = 80$ km for this cable. This implies $T_z = 2.91 T_x$. The force vector points down at an angle of 19° from the vertical. Assume that the sheath/ribbon is 10° from the horizontal. This rotates the components of the anchor cable force, so that they are 9° from perpendicular to the ribbon, pulling upslope. For an angle of 9°, the force perpendicular to the ribbon is 6.3 times the tangential force. If the cable must relieve 400 kN (this is the force of a 10 kg/m sheath over 4 km of vertical travel), the deflection force perpendicular to the ribbon is 2.52 MN, causing the ribbon to deflect 0.25 degrees.

Anchor cables relieve stress if the angle of the ribbon from the horizontal is greater than the angle of the anchor cable from the vertical. This can be expressed as:

$$\frac{dz}{dx} < \frac{1}{G(z)} = \left(e^{\frac{2(z+z_0)}{H_c}} - 1 \right)^{-\frac{1}{2}} \quad (41)$$

If the relief cables come off the sheath continuously, the resulting sheath shape may be described with a continuous equation. The z and x coordinates are used for altitude and surface position on the curved equator. The deflection force per length perpendicular to the ribbon is the curvature times $m_r V_r^2$:

$$f = \left(\frac{\frac{d^2z}{dx^2}}{\left(\left(\frac{dz}{dx} \right)^2 + 1 \right)^{\frac{3}{2}}} - \frac{1}{(R_E + z) \left(\left(\frac{dz}{dx} \right)^2 + 1 \right)^{\frac{1}{2}}} \right) m_r V_r^2 \quad (42)$$

This force can be divided into vertical and horizontal components. Equating these forces to the weight of the sheath and the tension in the cables gives the characteristic shape of the incline sections of the Launch Loop:

$$\frac{d^2 z}{dx^2} = \frac{1 + \left(\frac{dz}{dx}\right)^2}{R_E + z} - \frac{a_g(m_s + m_r) \left(1 + \left(\frac{dz}{dx}\right)^2\right)^2}{m_r V_r^2 \left(1 - G(z) \left(\frac{dz}{dx}\right)\right)} \quad (43)$$

If the relief cables are brought away from the Loop to the side at angle Θ from the plane of the Loop (to absorb sideways wind forces, for example), the $G(z)$ term in equation (43) is divided by $\cos(\Theta)$.

If $\frac{dz}{dx} = 0$, equation (43) may be reduced to:

$$\frac{m_s}{m_r} = \left(\frac{V_r}{V_o}\right)^2 - 1 \quad (44)$$

This is just the track to ribbon mass ratio implied by equation (2).

The ideal incline is as short as possible; this implies a steep starting angle. While equation (41) forces the slope to be less than a certain amount, the vertical height of the deflection ramp at the ends sets an even stiffer requirement on the starting angle. The vertical height of the deflection ramp is given by $z_D = R_D (1 - \cos(\alpha_0))$. If the deflection radius is 14 km, a starting incline angle of 20 degrees results in a change in vertical height of 850 m. This ramp can be placed below the surface, but it is still quite an engineering feat. A 30 degree deflection ramp changes height by 1880 m; a lot of added expense for a slightly shorter incline.

Assume a ribbon mass of 3 kg/m and a track and sheath mass of 10 kg/m. The cables have a characteristic length H_c of 80 km, and their angle from horizontal at the ground is 39 degrees ($z_0 = 20$ km). They are angled at 45 degrees from the plane of the Loop. These assumptions result in the incline shape plotted in Figure 7.

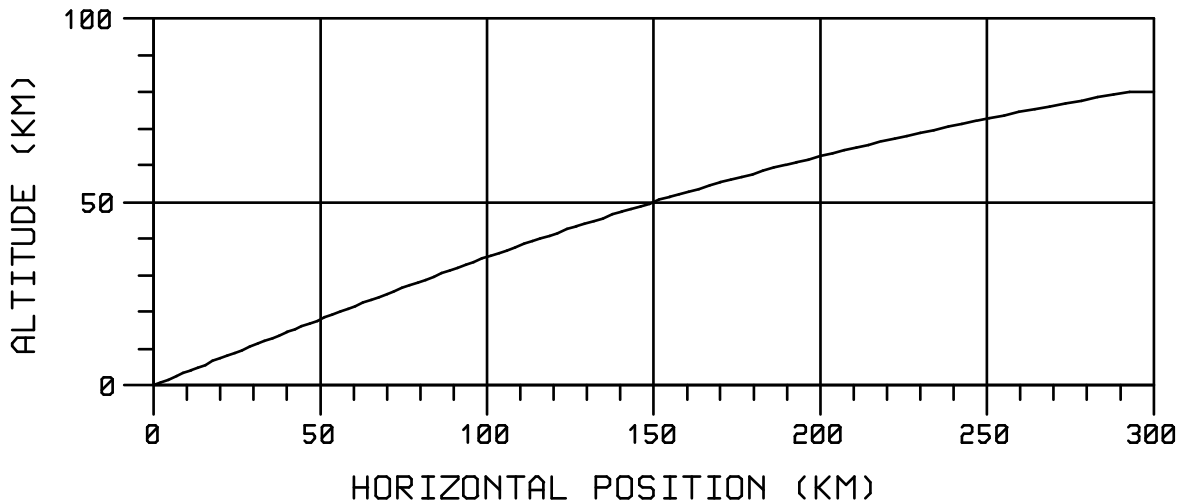


Figure 7. Altitude versus horizontal distance for a typical incline section.

12. Incline Sheath Construction

The incline sections are surrounded by two sheaths to protect the moving ribbon from the atmosphere. The outer sheath must be able to maintain high vacuum against mechanical stresses and diffusion from sea level atmosphere. A 10 cm outside diameter allows a large vacuum channel to the nearest pump. The sheath is made with Teflon-coated Kevlar fabric and epoxy-impregnated carbon fiber hoop spreaders spaced 10 cm apart. The outer sheath is covered with a Kevlar-mylar fabric, coated on the inside with 100 microns of aluminum, making it impermeable to gas diffusion.

The inner sheath must withstand full atmospheric pressure if the outer sheath is breached. It is made of 2mm thick aluminum, and has a rectangular cross section enclosing the ribbon and the support magnets.

Figure 8 shows a possible cross section for the incline sheath:

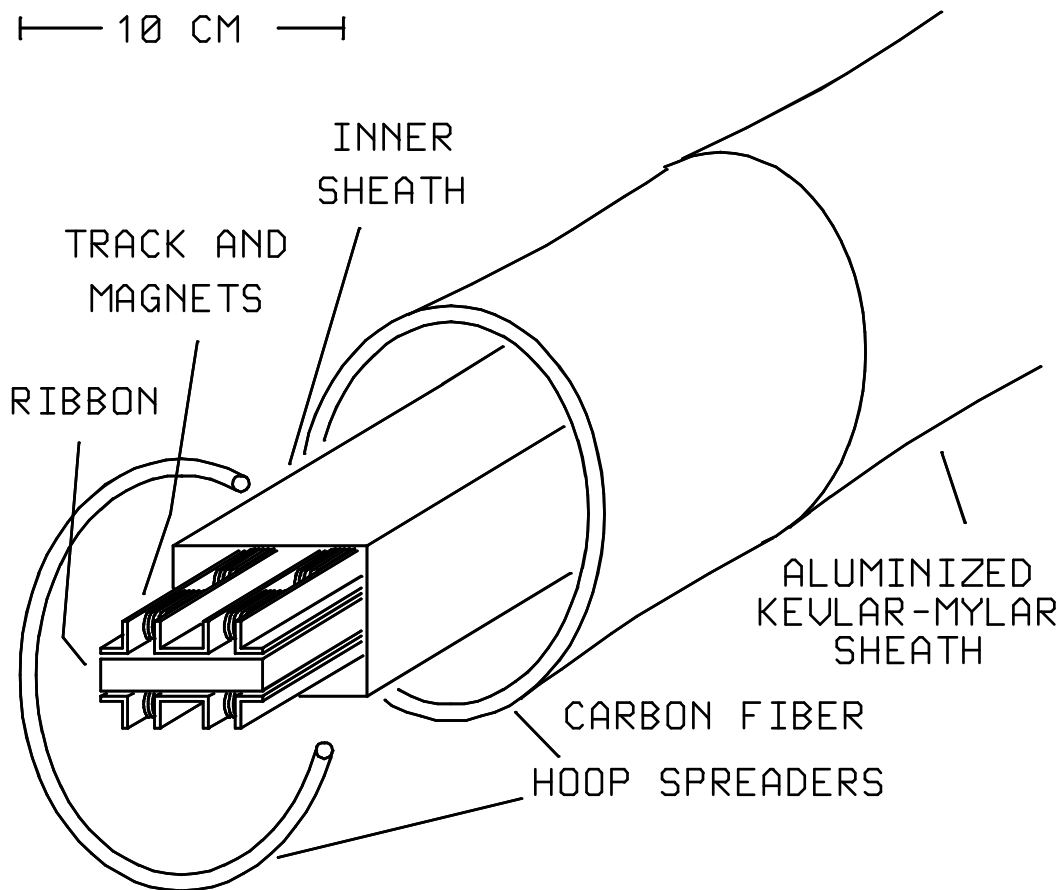


Fig. 8. Cross section of the incline sheath

The sheath weight of 100 N/m, plus wind loadings up to 50 N/m, are transmitted to the ribbon with magnets with a lift-to-weight ratio of 3. The resulting magnet weight is approximately 5 kg/m. Much better magnets may be possible.

The inclines may be struck by lightning. A lightning stroke can carry currents of up to 100,000 amps [15]; this current is carried by the outer and inner sheath, and the support cables, to the ground. The pulse propagates in both directions along the sheath. To keep the current from flowing all the way up to the station, the sheath is insulated at 30 km altitude (above the charge center of storm clouds) and support cables

provide a current return to ground.

The aluminum inner sheath has an electrical resistance of 2.5 mΩ per meter, so 130 volt-per-meter drops can be expected along the inner sheath from a lightning current pulse. The sheath to 10 km altitude is 30 km long, so the voltage drop can exceed 4 million volts. The controller interconnections must be designed with this in mind. Some of the lightning discharge current must be transmitted to the ribbon, to induce a similar voltage drop there, or arc-overs will occur. A lightning stroke transmits a negative charge to the ground, so the current to the ribbon may be transmitted by thermionic cathodes inside the sheath. Since cathode current emission densities of only 3 amp/cm² can be expected [16], a few hundred amps in the ribbon must be sufficient to induce voltage drops of 130 volts per meter. This implies a high longitudinal resistance (over large distances) in the ribbon, and affects ribbon design.

13. Acceleration Track

The launch track and sheath system cover the prograde ribbon between the east and west stations. The weight of the launch track and sheath, plus that of the anchor cables, must be equivalent to 7.1 kg/m to put the proper curve on the system.

The mass budget for the track/ribbon system per meter is as follows:

Temporary erection sheath	700 g/m
Magnet structures	2400 g/m
Electronics, etc.	300 g/m
Other track weight	600 g/m
Kevlar® cable weight	1000 g/m
Other cable weight	2100 g/m
Total	7100 g/m

The ratio of track to ribbon mass will be used later; it is defined by $\mu \equiv m_s/m_r$ and is approximately 1.33.

14. Launch Loop Failure

Catastrophic failure of the Loop can be expected occasionally because of control failure, fatigue, weather, improper vehicle handling, or major breaks in the sheath. It is important that the ribbon can be dumped from the track in a way that is not damaging to the structure or to the environment. 1.5×10^{15} J is enough energy to boil 400,000 m³ of seawater. This is equivalent to 30,000 tons of burning oil, or about 10% of the capacity of a modern supertanker. For safety reasons, Launch Loops must not be constructed near populated areas.

There should be provisions for parachutes on the upper deflection stations and portions of track and cable, so that these may be recovered if the Loop falls down. Lastly, spares for everything that can fall should be kept on hand, to minimize reassembly time. These measures increase the operating cost of the Launch Loop.

15. Collision Rates with Space Junk

Meteoroids and orbiting space debris can collide with the Launch Loop track and break it. Meteoroids come from random directions, and are not often in circular Earth orbits; the Loop has only one

chance to collide with them before they fall below it. The flux rate of particles large enough to seriously damage the Loop is too low to pose a hazard [11].

Orbiting space debris from human activity in space is in a decaying, near-circular orbit by the time it reaches Launch Loop altitudes. As the orbiting debris has many chances of collision, it poses a greater threat.

Assume that there is a steady "rain" of debris objects with mass M_d , effective drag area A_d and collision radius R_d spiraling in from nearly circular orbits at a rate of N_d . The atmospheric drag on an object is given by the form drag, which results in a power loss of:

$$\frac{\partial E}{\partial t} = \frac{1}{2} \rho_A A_d V_o^3 \quad (44)$$

This energy loss lowers the orbital altitude over time. The change of energy with altitude h is given by:

$$\frac{\partial E}{\partial h} = \frac{1}{2} M_d a_g h \quad (45)$$

where a_g is the gravitational acceleration.

The change in altitude with time can be derived as:

$$\frac{\partial h}{\partial t} = \frac{A_d \rho_A V_o^3}{M_d a_g} \quad (46)$$

R_s is the radius of the track and ribbon. All objects between $(R_d + R_s)$ and $-(R_d + R_s)$ can potentially hit one of the two tracks. Thus, the number of objects N that *might* hit the Loop are in a shell $4(R_d + R_s)$ thick; that number is:

$$N = 4(R_d + R_s) \frac{\partial t}{\partial h} N_d = \frac{4(R_d + R_s) M_d N_d a_g}{A_d \rho_A V_o^3} \quad (47)$$

Each of these objects crosses the equator twice per orbit, at a velocity V_o , independent of orbital inclination. The flux rate past the equator is thus:

$$\frac{dN_E}{dt} = \frac{NV_o}{\pi R_E} \quad (48)$$

where R_E is the radius of the Earth. An equatorial Loop intercepts a fraction of these proportional to its length:

$$\frac{dN_L}{dt} = \frac{L_{LOOP}}{2\pi R_E} \frac{dN_E}{dt} \quad (49)$$

The resulting collision flux is:

$$\frac{dN_L}{dt} = \frac{2(R_d + R_s) L_{LOOP} M_d N_d a_g}{A_d \rho_A \pi^2 R_E^2 V_o^2} \quad (50)$$

The form of equation (50) suggests that after a given amount of mass $MMTF$ (Mean Mass To Failure) passes through the altitude of the Loop, there will be a collision. Using the identity $V_o^2 \equiv R_E a_g$, we can take the inverse of equation (50) to get the $MMTF$:

$$MMTF = \frac{A_d \rho_A \pi^2 R_E^3}{2(R_d + R_s) L_{LOOP}} \quad (51)$$

Assume that a typical piece of space debris is a bolt with a drag area of 1 cm² and a radius of 1 cm. For a Loop at 80 km altitude, the orbital radius is 6450 km and the atmospheric density is 1.9×10^{-5} kg/m³. The Loop radius is 5 cm. The result is a $MMTF$ of 2×10^7 kg. While this seems like a large amount,

remember that one Launch Loop system at full power can launch that much mass into space in two days.

The high launch rates allowed by the Launch Loop requires that users act responsibly and not litter the regions of space near the Earth. The low launch costs of the Launch Loop will make garbage collection missions affordable. Users will have no excuse to leave radar detectable fragments in orbit, and will be liable if they do.

16. Drag Effects in Near-Earth Space

A major loss in the Launch Loop system is gas drag on the moving surface of the ribbon. Gas drag on the vehicle is also a problem, requiring vehicle launches at slightly higher velocity than would otherwise be necessary. This drag is the main reason the launch path is elevated to high altitudes.

A very thin, pumped sheath surrounds the ribbon, with pumping stations spaced at 10 km intervals along the launch track. This sheath allows the ribbon to move in a very high vacuum. Because the sheath is thin, it is easily punctured by meteoroids and debris, and ambient air can pour through a breach into the sheath. Fortunately, the movement of the ribbon helps move gas from a breach to the nearest pumping station.

A major breach may be as large as the cross sectional area of the sheath, about 20 cm². The air pressure at 80 kilometers altitude is 0.11 Pa, and the density is 1.9×10^{-5} kg/m³ [17]. Gasses flow through this breach at a pressure-driven rate of $A(2\rho P)^{\frac{1}{2}}$, or 4.1×10^{-6} kg/s.

Gasses move down the sheath at V_a , dependent on internal sheath structure. If $V_a \approx 0.25V_r$, there is about 6×10^{-10} kg of gas per meter of sheath, yielding a gas density of 6×10^{-7} kg/m³ inside the sheath. The mean free path is approximately 20 cm, justifying a free-molecule treatment of the problem.

Assume a worst-case wall accommodation coefficient of unity; that is, all molecules scatter from impacting the ribbon or sheath. The skin friction on the ribbon (with a long mean free path) is given by the particle flux rate times the energy gained per particle collision [14]:

$$Power \approx \frac{A\rho_A(V_r - V_a)^2 V_{th}}{(24\pi)^{1/2}} \quad (52)$$

Assume the thermal velocity V_{th} is 5000 m/s, the energy per molecule is 4 eV and the equivalent temperature is 30,000°K, heated by friction.

If pumping stations are spaced at 10 km intervals, up to 1000 m² of ribbon may be exposed. The drag loss from equation (52) is 40 Mw. This heats the ribbon by 1.6°K. While such a major breach should be sealed to save power, it will not cause the Launch Loop to fail.

Even if the sheath is not breached, the normal ambient gas density in the sheath causes drag. If the gas pressure is 0.01 Pa, and the gas temperature is 30,000°K, the gas density in the sheath is 1.2×10^{-9} kg/m³ and the drag loss on 5.2×10^5 m³ of ribbon is 40 Mw. While much better vacuums are possible; there is a tradeoff between pump cost and power cost.

A more important problem may be sputtering. If an iron atom is knocked loose at 14 km/s, it has an energy of 60 eV when it hits the sheath wall. This may be enough to sputter loose another atom, which collides with the ribbon, and so forth - the result may be a cascade of particles. For this reason, it is a good idea to coat the ribbon and the sheath wall with a material with low atomic weight and a low sputter yield; nitriding the surfaces, for example.

17. Vehicle Atmospheric Drag

Atmospheric drag on the vehicle causes power losses, and requires a higher terminal velocity on the vehicle to punch through what remains of the atmosphere.

For a vehicle with an effective frontal area of A_p , the vehicle drag power is given by:

$$Power = \frac{1}{2} \rho_A A_p V_p^3 \quad (53)$$

Where ρ_A is the air density at altitude. This can be integrated over the launch path to yield the lost drag energy E_{D0} :

$$E_{D0} = \frac{\rho_A A_p V_p^2 L_{LOOP}}{4} \quad (54)$$

After the vehicle leaves the Loop, it climbs out of the atmosphere in an elliptic orbit. The drag acceleration a_D as a function of altitude is:

$$a_D = \frac{\rho_0 e^{-z/H_A} A_p V_p^2}{2M_p} \quad (55)$$

The altitude as a function of horizontal distance is:

$$z = \frac{x^2}{2R_E} \left(1 - \left(\frac{V_o}{V_p} \right)^2 \right) \quad (56)$$

The equations can be combined and integrated to yield:

$$E_{D1} = \frac{(2\pi R_E H_A)^{\frac{1}{2}} \rho_0 A_p V_p^2}{4 \left(1 - \left(\frac{V_o}{V_p} \right)^2 \right)^{\frac{1}{2}}} \quad (57)$$

Assume a vehicle weighing 5000 kg with an effective frontal area of 2 m² is launched to a velocity of 10,500 m/s. The atmospheric drag forces from an 80 km launch result in a deceleration of 0.5 m/s², and energy losses of 0.8% on the Loop and 0.5% on the way out of the atmosphere. These are acceptable losses. If the launch track is positioned at higher altitudes, losses can be reduced, but the system is exposed to more collisions with space debris.

18. Launching Vehicles

A typical five-metric-ton vehicle is shown in Figure 9. The vehicle is equipped with rocket engines for orbital circularization at apogee, a lifting shell, and a heat shield and parachutes for emergency reentry of passengers. Magnets hold the vehicle off the ribbon using eddy current repulsion. Cheaper containers may be used for expendable cargo.

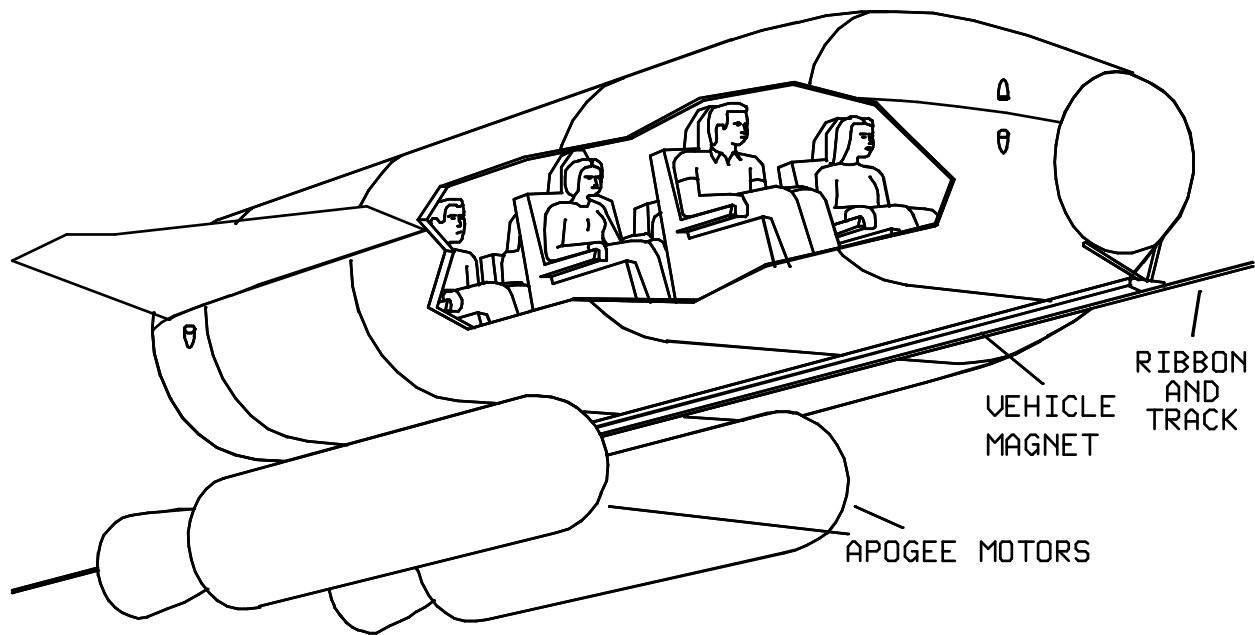


Figure 9. A typical 5 ton passenger vehicle, with magnets, rocket motors for apogee orbit insertion and a heat shield for accidental reentry.

The 10 meter long magnet racks on the vehicle generate a lift force of 50 kN and a drag force of 150 kN on the ribbon, which holds the vehicle up against gravity and accelerates it at 3 g's. With the vehicle near rest velocity, the ribbon is decelerated 3.6 m/s, and deflected downwards 1 m/s, an angle of 90 microradians. As the vehicle accelerates, the speed relative to the ribbon drops, decelerating the ribbon by 14 m/s at a vehicle speed of 10.5 km/s.

Tension must be released on the station anchor cables at either end of the launch track to compensate for the weight of the vehicle. At the beginning of acceleration, the 90 microradians of deflection under the vehicle is matched by a reduction of 90 microradians at west station. As the vehicle moves east, the west station deflection increases and the east station deflection decreases. As the vehicle approaches orbital velocity, the sum of station deflections increases, since the Loop is supporting less vehicle weight.

The deflection of the ribbon and track is illustrated in Figure 10. The following analysis is performed in the vehicle's frame of reference.

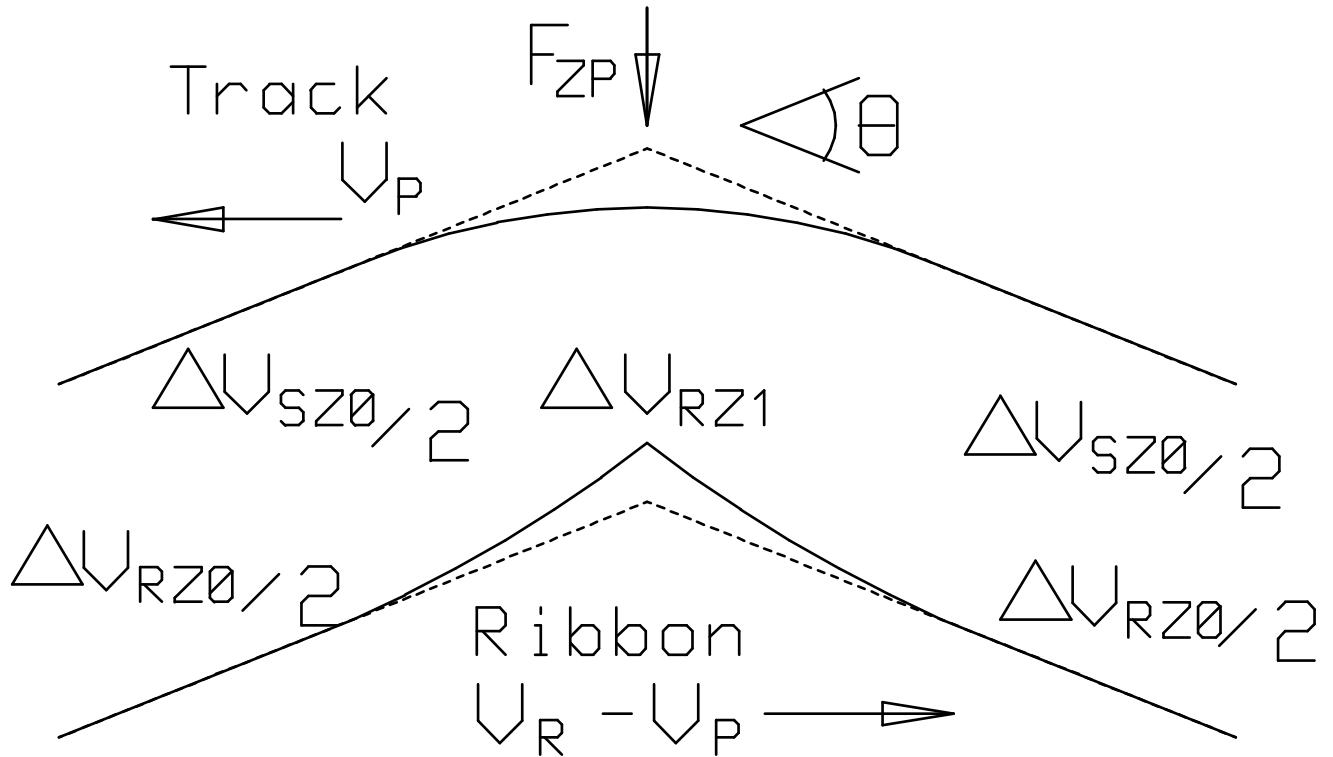


Figure 10. The deflection of ribbon and track as the y pass by the vehicle.

The downwards impulse force on the ribbon, and indirectly on the track, is given by:

$$F_{zp} = a_g M_p \left(1 - \left(\frac{V_p}{V_o} \right)^2 \right) \quad (58)$$

where V_o is circular orbit velocity.

Under the vehicle, this force is absorbed by a change in vertical ribbon velocity of ΔV_{rz1} . The change in velocity is:

$$\Delta V_{rz1} = \frac{F_{zp}}{m_r (V_r - V_p)} \quad (59)$$

The track, being uncoupled from the vehicle, experiences no sudden change in velocity, but is slowly accelerated by the control magnets. Part of the ΔV is coupled from the ribbon to the track, resulting in a vertical change in ribbon velocity of ΔV_{rz0} and the track by ΔV_{sz0} . From geometric considerations, these velocities are related by the angle Θ that the track is deflected:

$$\Theta = \frac{\Delta V_{rz0}}{V_r - V_p} = \frac{\Delta V_{sz0}}{V_p} \quad (60)$$

The force is given by:

$$F_{zp} = m_r \Delta V_{rz0} (V_r - V_p) + m_s \Delta V_{sz0} V_p \quad (61)$$

Define the track mass parameter $\mu \equiv m_s/m_r$. Equations (60) and (61) can be solved for ΔV_{rz0} and ΔV_{rs0} :

$$\Delta V_{rz0} = \frac{F_{zp}(V_r - V_p)}{m_r((V_r - V_p)^2 + \mu V_p^2)} \quad (62)$$

$$\Delta V_{sz0} = \frac{F_{zp}V_p}{m_r((V_r - V_p)^2 + \mu V_p^2)} \quad (63)$$

The change in velocity is the result of control magnet forces between track and ribbon over a horizontal region x_c to each side of the vehicle. The force in this region is a fraction χ of the track-to-ribbon attraction force. χ is limited in one direction because the track and ribbon cannot repel each other ($\chi > -1$). In the other direction, χ is limited by the maximum force the control magnets can generate, and the peak power the power control devices can handle.

Since the track and the ribbon do not follow the same path, the spacing between them changes. If the spacing becomes too great, the control magnets are unable to compensate, and the system falls apart. If the spacing becomes zero, the track crashes into the ribbon.

The spacing change is a function of vehicle mass and velocity, and track and ribbon mass per length. For a given maximum spacing change and vehicle mass, there is a minimum ribbon mass. This one consideration scales the mass of the ribbon, and indirectly the rest of the Launch Loop.

Define the two variables $\alpha \equiv V_r/V_o$, and $\beta \equiv V_p/V_o$. The length of the region disturbed by a payload passage can be expressed as:

$$\Delta x = \frac{1}{\chi} \left(\frac{M_p}{M_r} \right) \left(\frac{\beta^2(1 - \beta^2)}{(\alpha - \beta)^2 + \mu\beta^2} \right) \quad (64)$$

and the change in vertical spacing is:

$$\Delta z = \left(\frac{M_p}{m_r} \right)^2 \left(\frac{a_g}{8\chi V_o^2} \right) \left(\frac{\beta}{\alpha - \beta} \right)^2 \left(\frac{(1 - \beta^2)^2}{(\alpha - \beta)^2 + \mu\beta^2} \right) \quad (65)$$

There is a vehicle velocity V_p between 0 and V_o where equation (65) is maximized. This is the velocity at which the ribbon is pulled farthest from the track by a payload passage. Given $\mu = 2.0$ and $\alpha = 1.75$, the equation is maximized with a $\beta \approx 0.658$. The maximum deflection for the parameters given is:

$$\Delta z_{\max} = \left(\frac{M_p}{m_r} \right)^2 \left(\frac{0.0071 a_g}{\chi V_o^2} \right) \quad (66)$$

Given $\chi = -0.5$, a 5 metric ton payload, and a ribbon mass of 3 kg/m, the spacing change is -0.5 cm. The disturbance spreads over a 420 meter region of the ribbon-track system.

A vehicle traveling faster than V_o generates an upwards force. Almost all of this force is eventually provided by the deflection of the track, requiring a very strong coupling force between the ribbon and track. If a 5000 kg payload is traveling at 10.5 km/s relative to the Loop, a χ of 36 is needed to maintain a spacing change of 0.5 cm; that is, 36 times the normal attractive force. The track-ribbon region affected is about 40 meters long; the higher force is required for about 5 milliseconds.

The passage of the 10 meter long vehicle support magnet also induces oscillations in the ribbon segments. As the forward end of a segment passes into the magnet field, it slows before the back end does, compressing the segment. When the compression wave reaches the back end of the segment, it is reflected as a tension wave, and the segment oscillates. A similar tension wave is started when the segment passes the front of the vehicle. This second wave can add constructively or destructively to the previously generated wave. The stretch in the segment is worst when the speed difference between vehicle and ribbon is the

speed of sound in the ribbon material, which occurs when the vehicle speed is about 6 km/s. The speed of sound in the ribbon material is C , the magnet length is L_M , and the segment length is l_{seg} . The maximum compression or stretch in the ribbon is:

$$stretch = \frac{a_p M_p l_{seg}}{2m_r L_M C^2} \quad (67)$$

This value of stretch occurs if the end effects add constructively. For the current design, the maximum segment stretch is 0.014%. This effect can be minimized by making L_M an even multiple of l_{seg} , so that the waves add destructively.

Sudden introduction of vehicle forces on the ribbon at west station can also have a bad effect on the ribbon. A sudden slowing down of the ribbon affected by the vehicle can make it separate from the ribbon ahead of it. The vehicle acceleration should be increased gradually to prevent this.

If the payload force is increased from zero to $a_p M_p$ over time t_s , and L_L is the length of the Launch Loop from the west station to the east motor, the total stretch of the ribbon is:

$$stretch = \frac{a_g M_p L_L}{m_r V_r^3 t_s} \quad (68)$$

Ten seconds is allowed to change the acceleration from 0 to 30 m/s². The ribbon velocity change of 3.6 m/s is spread over 140 km of ribbon. This results in a 0.4% stretch by the time the ribbon reaches the motors at the east end, where the velocity is restored. The ribbon may be "pre-accelerated" by the east end motors in anticipation of a payload launch, cutting the stretch in half.

A problem can also occur at the east end of the launch path, as the vehicle is nearing ribbon speed. The ribbon is decelerated by up to 15 m/s; to get this portion of the ribbon back up to speed requires a power input of 9 gigawatts. If the velocity change is spread out over the ribbon to minimize stretch, the affected section of ribbon may be brought up to speed by multiple passes through the motors.

Vehicles can also be launched in "burst mode". Velocity changes are averaged out over the ribbon if vehicles are launched in rapid succession and at just the right rate. The entire ribbon may be slowed perhaps 50 m/s by such a burst. The support capability of the ribbon is lowered by only 1%, causing the cable tension at the surface to drop about 30%. A ribbon ΔV of 50 m/s can launch a burst of 15 vehicles in 6 minutes. The velocity may be restored slowly with low power motors.

19. Ribbon Cooling

Vehicle drag results in ohmic heating of the ribbon. The heat is stored in the ribbon and carried away from the vehicle, then dissipated by black body radiation from the hot ribbon to the inner sheath wall. The heat removing capacity of the ribbon is proportional to $V_r - V_p$ and decreases with vehicle speed; fortunately drag dissipation is proportional to the same factor.

If the ribbon heats up past the Curie temperature of iron, 1000°K, it stops behaving as a magnetic material, and the control magnets fail. Vehicles should not be launched faster than the ribbon can cool itself.

The temperature change of the ribbon as it passes under the vehicle is:

$$\Delta T = \frac{a_p M_p}{\delta W \rho_{Fe} C_{Fe}} \quad (69)$$

where W is the width and δ is the thickness of the iron ribbon, which has a density of ρ_{Fe} (7880 kg/m³) and a heat capacity of C_{Fe} (600 J/kg-°K). A five ton vehicle accelerating at 3 g's changes the ribbon

temperature by 84°K.

The ribbon thermal dissipation per length is given by:

$$\frac{\partial P}{\partial x} = 2W\varepsilon\sigma_B (T_r^4 - T_s^4) \quad (70)$$

where ε is the emissivity and σ_B is the Stephan-Boltzmann black body constant ($5.67 \times 10^{-8} \text{ w/m}^2 \cdot \text{K}^4$). T_r is the ribbon temperature and T_s is the background temperature. If the power dissipation is 350 Mw, ε is 0.8, and T_s is 300°K, the average ribbon temperature is 380°K.

Over time, the heated ribbon radiates and cools. The change in ribbon temperature with time is given by:

$$\frac{dT_r}{dt} = - \left(\frac{\varepsilon\sigma_B}{\rho_{Fe}C_{Fe}\delta} \right) (T_r^4 - T_s^4) \quad (71)$$

The ribbon sheds heat much more efficiently at high temperatures. Near 1000°K, the ribbon temperature drops 85°K in 45 seconds. This places a thermal limit of 80 evenly-spaced payloads per hour on this size of Launch Loop.

Using equation (71), the temperature profile of the Launch Loop ribbon during a 15-vehicle, 24-second-spaced burst mode launch can be computed, and is illustrated in Figure 11. The temperature reaches nearly 1000°K. Another such burst cannot be repeated for half an hour, although shorter bursts can be more frequent.

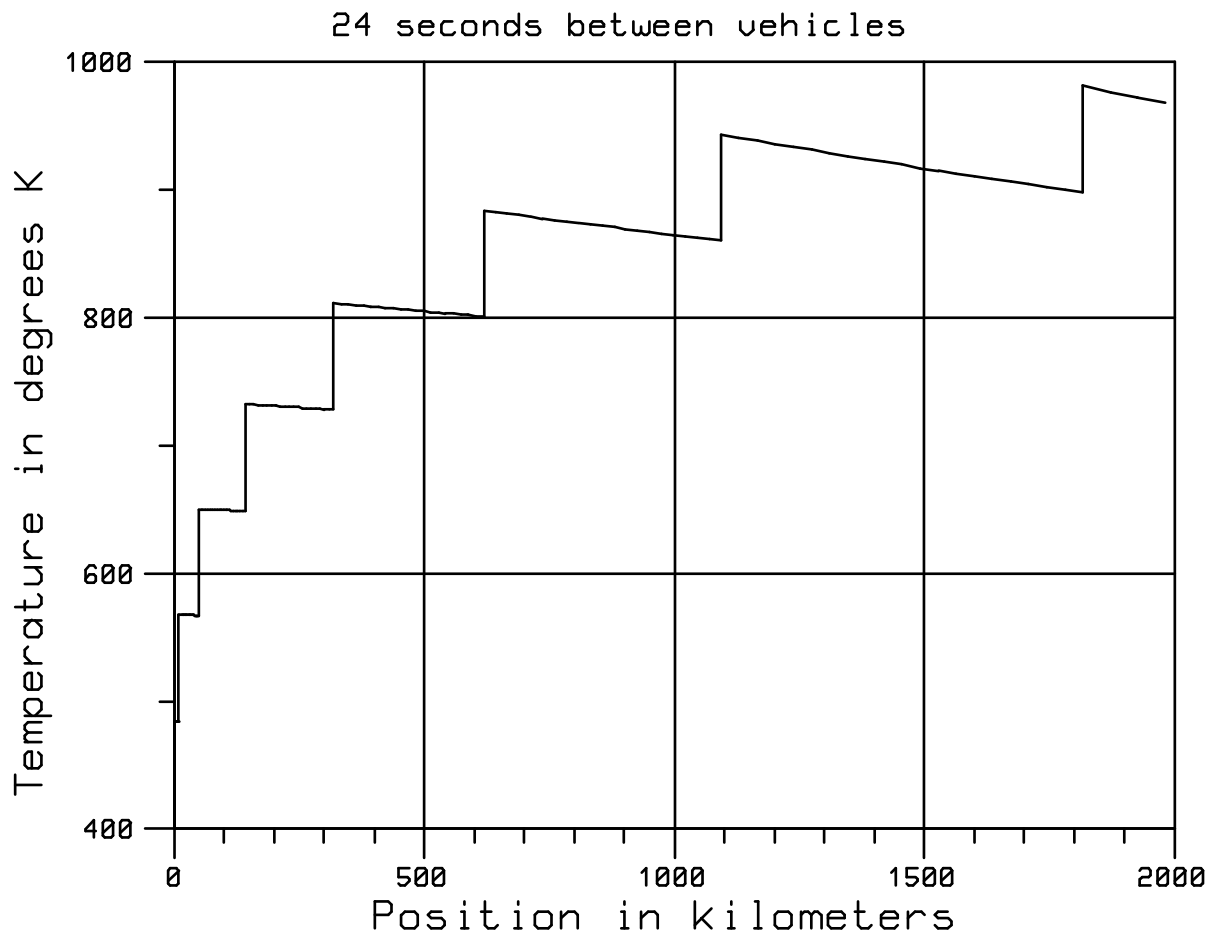


Figure 11. Temperature profile of the Launch Loop ribbon during a burst launch.

20. Energy and Power Use by the Launch Loop

The vehicle is accelerated by ribbon drag, and the total kinetic energy removed from the ribbon is more than twice the resultant vehicle kinetic energy. A 5 ton vehicle launched at 10.5 km/s removes 735 GJ of kinetic energy from the ribbon, slowing it down by 3.6 m/s at the start of acceleration and 14.3 m/s at the end. This energy is put back in by a high-efficiency linear induction motor located on the surface near the eastern turnaround. This motor is driven by a 150 kHz source and is 10 km long, with 1 million ferrite cores for poles. The motor supplies power to the ribbon which in turn drives the generators on the low acceleration section magnets; it also makes up for drag caused by residual gasses in the sheath.

The track magnet power consumption is about 40 Mw, and the deflectors consume about 100 Mw. Drag from residual gasses and magnetic field discontinuities consumes about 60 Mw. If a 500 Mw power generator is available, then 300 Mw is available for restoring losses from vehicle launches. This allows the launch of 35 five-ton vehicles per day to near escape velocity, or 48 per day to low earth orbit.

To launch at maximum rate, a much larger power plant is needed. To launch 5 ton vehicles to near-escape velocity at the high rate of 80 per hour requires a 17 Gw power plant. This one minimum-sized Launch Loop can serve two very different sized launch markets.

The power from the generators is put into the ribbon of the Loop with 10 km long, high-efficiency linear induction motors. The motors may be analyzed like those planned for high-speed surface trains [10]. Launch Loop motors are longer, narrower, higher power, and much higher velocity, resulting in efficiencies approaching 100%. The short motor wavelengths and high speed requires high frequency, switched-mode power supplies. This results in more costly drive electronics than the line-frequency power switches used for normal motor applications. The costs and driver efficiencies are similar to those of large, high-efficiency switched power supplies.

21. Construction and Operating Costs

A detailed estimate of the costs involved would be premature, but some costs can be at least identified, or compared to existing construction projects.

The following analysis does not include the cost of apogee insertion motors, payload shrouds, communication packages, or other per-vehicle costs. Nor does it include the reduction in useful payload weight caused by the weight of these items.

The following costs have been found:

600 metric tons carbon fiber at \$25/kg	\$ 15.0M
6000 metric tons Kevlar® aramid fiber at \$25/kg	\$150.0M
1500 metric tons Alnico 8, at \$40/kg, formed	\$ 60.0M
11 ea. 56 Mw dual FT4 power plants at \$7M ea	\$ 77.0M
500 MW motor power switchers	\$ 50.0M
1 million ferrite motor cores, at \$3 each	\$ 3.0M
470,000 low power track controllers, at \$100 each	\$ 47.0M
50,000 high power track controllers, at \$1000 each	\$ 50.0M
150,000 D magnet controllers, at \$800 each	\$120.0M
	\$572.0M

(\$100 per control package and \$0.10 per average watt assumed)

Other costs can be identified, such as sheath manufacturing, magnet winding, ramps, pumps, and so forth. The cost of floats and anchoring cables to the seabed are unknown.

Assume the total cost of the Launch Loop, including research costs, comes to 2 billion dollars. If it is used at only 30% capacity of 500 Mwe (26,000 metric tons per year), and is amortized over 1 year as a high-risk venture, the cost per gross kilogram (including 6 cents per kwhr oil fuel cost) is \$85. While this launch rate is nearly two orders of magnitude above present U.S. launch rates, it is a tiny fraction of the 3.5 million tons per year capacity of the basic system.

Later, at 85% usage of a 4 Gwe power capacity (750,000 tons per year), 5 year amortization, 9 billion dollar capital cost, and 1.3 cents per kwhr fuel cost, the cost per gross kilogram is \$3. At this cost, labor and vehicle systems will probably dominate net payload cost.

Total Launch Loop system cost is likely to be well below that of Earth-to-high-orbit rocket systems.

21. Possibilities

This version of the Launch Loop launches 5 metric ton vehicles from the Earth to geosynchronous, LaGrange, and lunar destinations, but other applications are possible.

Launch Loop throughput, size and speed are limited only by economics; the ribbon can be made wider or longer, and more ribbons can be added to the side. More Launch Loops can be built elsewhere on the equator.

A smaller, lower-speed Loop with a parabolic shape may be built for the "first stage" of a rocket system. For equivalent payloads to orbit, this lower speed Loop must carry heavier loads, and is more subject to wind loading and ribbon stretching with altitude.

The speed of the Loop may be increased, opening the rest of the solar system to this form of launch. A Loop running at ribbon speeds of 18 km/sec can send vehicles directly to Venus, Mars, the asteroid belt, and Jupiter. Other destinations may be possible with planetary assist maneuvers. Efficiency is low for lower ΔV missions, however.

The present scheme for the Launch Loop includes two expensive and power-consuming 180° deflectors. The deflectors can be eliminated by a Loop that encircles the Earth, brought down to the ground at appropriate intervals, or running entirely in orbit with periodic anchor cables and elevators. Such a launch system would be constructed from orbit [5,6].

The Launch Loop may be used for other purposes, as well. The low ratio of dissipation to energy storage make the Loop an effective form of energy storage for power grids, and an interesting method of transmitting power over long distances. Power can be transmitted for 5000 km with less than 1% loss. Similar superconducting ring structures are being considered [14].

Lastly, Launch Loops may be constructed off Earth. A 200 km Launch Loop on the Moon can be operated entirely on the surface, without elevating ramps. Accelerations would be lower than present mass driver designs, and the Launch Loop would be easier to construct. Launch Loops can be built on orbiting structures, providing in-space transportation without expending reaction mass, if traffic in all directions is properly balanced. Passive capture ribbons can be placed on orbiting structures for capturing material launched from Earth and Moon.

Conclusions

More study remains to determine the details of a Launch Loop operation; the idea may prove impractical because of instabilities, expense, or political obstruction. Regardless of its success, it is hoped that others are stimulated to think of low-cost approaches to Earth launch using existing physics and existing engineering materials.

The rocket has served us well during the last few decades, and will continue to find uses in new applications and at the frontiers of space. The traffic necessary to justify even a minimum scale Launch Loop must be established before its construction. Rocket launch vehicles are establishing this market. Low-cost space utilities such as the Launch Loop will replace rockets in high volume applications, making space settlement and industrialization economically practical.

Acknowledgements

Special thanks to Dick Pilz and Dana Johansen for help with the mechanical engineering. Roger Arnold, Paul Birch, Ken Brakke, John Cousins, Eric Drexler, Robert Forward, Eric Geislinger, John Hull, Malvern Iles, Donald Kingsbury, Earl Smith, and Grace Tsang provided general discussion and review. Indiana General, Union Carbide, DuPont, United Technologies Gas Turbine division, Hitachi Magnetics, Thomas and Skinner Magnetics, and the NOAA provided valuable data. The members and staff of the L-5 Society have been very helpful.

Very special thanks are due to Tektronix, Inc., and its managers for providing a working situation tolerant of after-hours studies such as this. Availability of graphics terminals and UNIX™ (a trademark of Bell Labs) made this paper possible.

References

- [1] "Future Space Transportation System Study," *Astronautics and Aeronautics*, Vol. 21, June 1983, pp. 36-56.
- [2] Chilton, F., Hibbs, B., Kolm, H., O'Neill, G. K., and Phillips, J., "Electromagnetic Mass Drivers," *Space Based Manufacturing from Nonterrestrial Material*, AIAA Progress in Astronautics and Aeronautics, Vol. 57, 1977, pp. 37-61.
- [3] Kolm, H., "Mass Driver Up-Date," *L-5 News*, Vol. 5, Sept. 1980, pp. 10-12.
- [4] Arnold, R., and Kingsbury, D., "The Spaceport," *Analog*, Vol. 99, Nov. and Dec., 1979.
- [5] Brakke, K., "The Skyrail," *L-5 News* July, 1982.
- [6] Birch, P., "Orbital Ring Systems and Jacob's Ladders," *Journal of the British Interplanetary Society*, Vol. 35, November 1982, pp. 475-497.
- [7] Moravec, H., "A Non-Synchronous Orbital Skyhook," *Journal of the Astronautical Sciences*, Vol. 25, No. 4, 1977.
- [8] Atherton, D. L., "Maglev Using Permanent Magnets," *IEEE Transactions on Magnetics*, Vol. MAG-16, Jan. 1980, pp. 146-148.
- [9] DuPont Bulletin K-2, "Characteristics and Uses of Kevlar® 49 Aramid High Modulus Organic Fiber," DuPont Textile Fibers Department, Technical Service Section, Wilmington, Delaware 19898.
- [10] Yamamura, S., *Theory of Linear Induction Motors*, Wiley, 1979, 2nd edition.
- [11] Vedder, J. F., "Micrometeoroids," *Satellite Environment Handbook*, Stanford University Press, 1965, 2nd edition.
- [12] Madden, R. A. and Zipser, E. J., "Multilayered Structure of the Wind over the Equatorial Pacific During the Line Islands Experiment," *Journal of the Atmospheric Sciences*, Vol. 27, March 1970, pp. 336-342.
- [13] O'Hanlon, J.F., *A User's Guide to Vacuum Technology*, Wiley, 1980.
- [14] Hull, J. R., "Magnetically Levitating Loop, A New Energy Storage Concept," Internal research paper, Argonne National Laboratory, April 1983.
- [15] Uman, M. A., *Lightning*, Dover, 1984.
- [16] *Reference Data for Radio Engineers*, International Telephone and Telegraph Corporation, 1956, fourth edition, p. 367.
- [17] *CRC Handbook of Chemistry and Physics*, 1982, 63rd edition, p. F166.
- [18] Lofstrom, K., "The Launch Loop," AIAA-85-1368, 21st Joint Propulsion Conference, 1985.
- [19] Lofstrom, K., "The Launch Loop," *Analog*, Vol. 103, Dec. 1983, pp. 67-80.